Anti-Noise Quantum Network Coding Protocol Based on Bell States and Butterfly Network Model

Zhexi Zhang[1] and Zhiguo Qu[1, 2, *]

Abstract: How to establish a secure and efficient quantum network coding algorithm is one of important research topics of quantum secure communications. Based on the butterfly network model and the characteristics of easy preparation of Bell states, a novel anti-noise quantum network coding protocol is proposed in this paper. The new protocol encodes and transmits classical information by virtue of Bell states. It can guarantee the transparency of the intermediate nodes during information, so that the eavesdropper Eve disables to get any information even if he intercepts the transmitted quantum states. In view of the inevitability of quantum noise in quantum channel used, this paper analyzes the influence of four kinds of noises on the new protocol in detail further, and verifies the efficiency of the protocol under different noise by mathematical calculation and analysis. In addition, based on the detailed mathematical analysis, the protocol has functioned well not only on improving the efficiency of information transmission, throughput and link utilization in the quantum network, but also on enhancing reliability and anti-eavesdropping attacks.

Keywords: Network coding, quantum network coding, bell states, butterfly network model, quantum communication, eavesdropping detection.

1 Introduction

In recent years, quantum secure communication has become one of important research hotspots in the field of information security due to its absolute security compared with classical communication [Yu and Pan (2014)]. So far, the development of quantum secure communication mainly focuses on quantum key distribution (QKD), quantum secret sharing (QSS), quantum secure direct communication (QSDC) and quantum identity verification (QIV). Among them, BB84 protocol proposed by Bennett and Brassard in 1984 proved the unconditional security of quantum communication [Bennett and Brassard (1984)]. In 1992, Bennett released a B92 quantum key distribution protocol [Bennett (1992)], etc. The intermediate nodes of the traditional classical network are only responsible for routing, but do not process the data, which will do nothing to improve the

[1] Jiangsu Collaborative Innovation Center of Atmospheric Environment and Equipment Technology, Nanjing University of Information Science and Technology, Nanjing, 210044, China.

[2] School of Computer and Software, Nanjing University of Information Science and Technology, Nanjing, 210044, China.

[*] Corresponding Author: Zhiguo Qu. Email: qzghhh@126.com.

efficiency of information transmission in the network. Instead, network coding is an information exchange technology that integrates routing and coding, which is of great significance for improving network transmission efficiency. There are abundant research achievements in quantum communication technology and quantum network encoding technology [Hayashi (2007); Hayashi, Iwama and Nishimura (2007); Shang, Zhao, Wang et al. (2014)], and the specific achievements are described as follows.

In terms of quantum secure communication, the relevant research [Bennett, Brassard, Crépeau et al. (1993); Moroder, Kleinmann, Schindler et al. (2013); Peng, Yang, Bao et al. (2005); Yin, Ren, Lu et al. (2013)] also indicated that large-scale network communication is an inevitable trend in the development of quantum communication. And the complexity of the large-scale structure of the network itself will lead to transmission congestion, which may contribute to problems such as low communication efficiency. As a result, it has practical significance to research the quantum network coding. In terms of quantum network coding, Hayashi et al. were the first to propose the concept of quantum network coding. Quantum network coding technology is mainly used to solve the bottleneck problem in quantum network. Hayashi et al. [Hayashi, Iwama and Nishimura (2007)] used the butterfly network model to achieve two arbitrary quantum states probabilistic cross transmission in 2006, which made the quantum network coding possible. They also proposed the famous XQQ protocol. In 2007, Hayashi combined quantum teleportation in the quantum network coding and designed the quantum butterfly network coding protocol based on the sender pre-shared entangled states. In 2009, Leung et al. [Akter, Lutfa, Natarajan et al. (2009)] implemented quantum network coding for various network models. In 2010, based on the results of Hayashi's research, Ma et al. [Ma, Chen, Luo et al. (2010)] proposed an effective implementation of m-qubit cross transfer protocol through senders sharing non-maximum entangled states. In 2012, Yan Shuaishuai et al. [Yan, Kuang and Guo (2012)] proposed a quantum network coding protocol to transmit 2-level quantum entanglements through two pairs of non-maximized GHZ entangled states shared between two senders as the transmission channel, which make the transmission in the butterfly network more efficiency. In 2013, Nishimura [Nishimura (2013)] defined the limits of the reachable rate in quantum network coding based on butterfly network.

From the quantum network coding achievements given, it's easy to know that quantum network coding technology has a great development prospect. It has become a research hotspot in quantum secure communication for secure and efficient information transmission. Additionally, some new researches on resisting quantum noise has emerged, in recent years. In 2010, Korotkov et al. [Korotkov and Keane (2010)] proposed a protocol to overcome decoherence by using quantum non-collapse measurements, which can preserve the quantum states effectively. In 2014, Guan et al. [Guan, Chen, Wang et al. (2014)] analyzed the remote preparation of two arbitrary quantum bits in the noise environment and calculated the effect of quantum noise on protocol efficiency. In 2015, Fortes et al. [Fortes and Rigolin (2015)] made a detailed analysis of the effect of noise on the quantum teleportation and concluded that the interaction between the two kinds of noises has some symmetry. In 2017, Wang et al. [Wang and Qu (2016); Wang, Qu, Wang et al. (2017); Wang, Qu, Wang et al. (2017)] conducted quantum noise analysis on quantum remote preparation of single particles, two particles and multiple particles, and gave the efficiency of some protocols in the noise environment respectively.

In this paper, a novel quantum network coding protocol based on butterfly network model and Bell states is proposed. The protocol takes Bell states as the carrier, codes and hides classical information by virtue of Pauli operators for improving the efficiency, throughput and link utilization of quantum network. The transparency of the intermediate nodes to the specific information transmitted, and the detection and eavesdropping in the transmission process also guarantee the reliability of the protocol and the ability to prevent attacks. In addition, we also analyze the efficiency of the protocol under noise, and find that the amplitude damping noise has the least impact on the channel, while the depolarizing noise has the greatest impact.

The arrangement of this paper is described below. Section 2 introduces the preliminary knowledge related to the new protocol, including butterfly network model, Bell states and Pauli operators. Section 3 introduces the main steps of the new quantum network coding protocol in detail. Section 4 analyses the effect of noise on the fidelity of communication. Section 5 provides security and resource consumption analysis. Finally, the conclusion is given in Section 6.

2 Preliminary

2.1 Butterfly network model

Butterfly network model [Wei and Cioffi (2002)] (Fig. 1) is a typical example of implementing maximum flow transmission, which can clearly indicate the advantages of network coding. As shown in Fig. 1, the source nodes S_1 and S_2 send 1 bit information a and b to the target nodes T_1 and T_2 respectively. All channels in the figure are set up to transmit 1bit information.

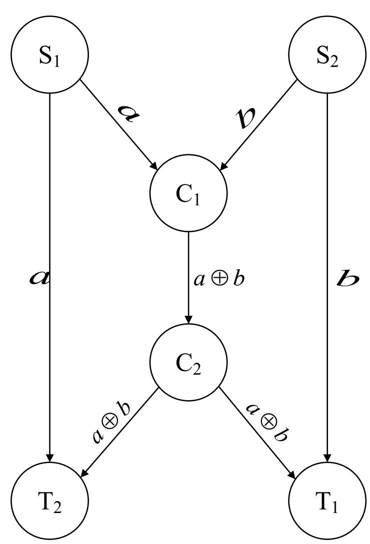

Figure 1: Butterfly network model

According to the max-flow min-cut theorem [Iri (2002)], the maximum transmission rate from the source node S_1 (S_2) to the target node T_1 (T_2) should be less than or equal to 2.

In the traditional network transmission, the node C_1 can only transmit 1 bit information to the node C_2 at one time, so the channel $C_1 \to C_2$ needs to be used twice, and C_2 also needs to transmit twice to the target node T_1 and T_2, the average transmission efficiency is 1.5 bit/unit time.

Through the network coding transmission, the node C_1 encodes information received from S_1 and S_2. The coding results $a \oplus b$ will be sent to the node C_2, and then node C_2 sent it to T_1 and T_2. The target node T_1 (T_2) obtains information b and $a \oplus b$ (a and $a \oplus b$), T_1 (T_2) can obtain the information a (b) from S_1 (S_2) by decoding $b \oplus (a \oplus b) = a$ ($a \oplus (a \oplus b) = b$). In this case, the average transmission rate is 2 bit/unit time, which achieves the network maximum flow value.

2.2 Bell states and Pauli matrices

Bell states are entangled states consisting of two particles. In a Bell state, the two particles are correlated, that is, the change of one particle will affect another particle. The four Bell states in the protocol are defined as follows:

$$\left|\Phi^+\right\rangle = \frac{|00\rangle + |11\rangle}{\sqrt{2}} = \frac{|++\rangle + |--\rangle}{\sqrt{2}} \tag{1}$$

$$\left|\Phi^-\right\rangle = \frac{|00\rangle - |11\rangle}{\sqrt{2}} = \frac{|+-\rangle + |-+\rangle}{\sqrt{2}} \tag{2}$$

$$\left|\Psi^+\right\rangle = \frac{|01\rangle + |10\rangle}{\sqrt{2}} = \frac{|++\rangle - |--\rangle}{\sqrt{2}} \tag{3}$$

$$\left|\Psi^-\right\rangle = \frac{|01\rangle - |10\rangle}{\sqrt{2}} = \frac{|+-\rangle - |-+\rangle}{\sqrt{2}} \tag{4}$$

Here, $|0\rangle$ and $|1\rangle$ are the eigen states of σ_Z, $|+\rangle$ and $|-\rangle$ are the eigen states of σ_X. It is easy to prove that { $\left|\Phi^+\right\rangle, \left|\Phi^-\right\rangle, \left|\Psi^+\right\rangle, \left|\Psi^-\right\rangle$ } constitute an orthogonal complete basis vector of a two quantum bits state system.

The quantum bits transmitted in the quantum communication network are encoded by unitary operators. The fundamental unitary operators operated on quantum bits are also refer to as quantum logic gates.

In this paper, four Pauli operators are used to encode classical information. The unitary operators operated on each particle of Bell states is the same, and each Bell state will become one of the four Bell states under the transformation of four Pauli operators. The four Pauli operators are given as follows:

$$I = \begin{pmatrix} 1 & 0 \\ 0 & 1 \end{pmatrix} = |0\rangle\langle 0| + |1\rangle\langle 1| = U_0 \tag{5}$$

$$\sigma_Z = \begin{pmatrix} 1 & 0 \\ 0 & -1 \end{pmatrix} = |0\rangle\langle 0| - |1\rangle\langle 1| = U_1 \tag{6}$$

$$\sigma_X = \begin{pmatrix} 0 & 1 \\ 1 & 0 \end{pmatrix} = |0\rangle\langle 1| + |1\rangle\langle 0| = U_2 \tag{7}$$

$$i\sigma_Y = \begin{pmatrix} 0 & 1 \\ -1 & 0 \end{pmatrix} = |0\rangle\langle 1| - |1\rangle\langle 0| = U_3 \tag{8}$$

The results of four Bell states under the transformation of four Pauli operators are shown in Tab. 1.

Table 1: Relations of four Bell states under the action of Pauli matrix

U_x \ Bell states	$\|\Phi^+\rangle$	$\|\Phi^-\rangle$	$\|\Psi^+\rangle$	$\|\Psi^-\rangle$
U_0	$\|\Phi^+\rangle$	$\|\Phi^-\rangle$	$\|\Psi^+\rangle$	$\|\Psi^-\rangle$
U_1	$\|\Phi^-\rangle$	$\|\Phi^+\rangle$	$\|\Psi^-\rangle$	$\|\Psi^+\rangle$
U_2	$\|\Psi^+\rangle$	$\|\Psi^-\rangle$	$\|\Phi^+\rangle$	$\|\Phi^-\rangle$
U_3	$\|\Psi^-\rangle$	$\|\Psi^+\rangle$	$\|\Phi^-\rangle$	$\|\Phi^+\rangle$

3 Quantum network coding protocol

As shown in Fig. 2, two senders S_1 and S_2 are required to send 2 bits of classic information to T_1 and T_2 respectively. Let suppose that S_1 transmit the classical information m_1, that is corresponding to the Pauli operator U_{m1}, while the classical information m_2 transmitted by S_2 is corresponding to the Pauli operator U_{m2}. Among them, the channels $S_1 \to T_2$, $S_2 \to T_1$, $S_1 \to C_1$ and $S_2 \to C_1$ transmit single quantum bit, and the channels $C_1 \to C_2$, $C_2 \to T_1$ and $C_2 \to T_2$ transmit two quantum bits, respectively.

The key of the quantum network coding based on the butterfly network model is combining the information of two senders at node C_1 by coding and then receivers jointly decode, and obtain the information to be transmitted.

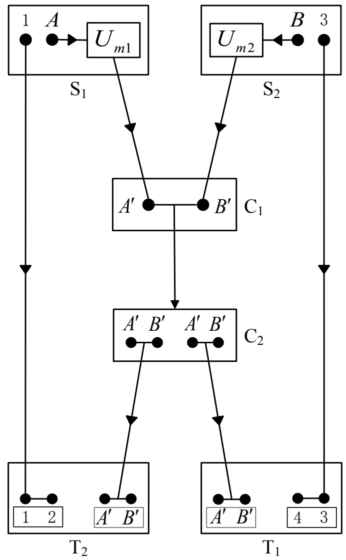

Figure 2: Diagram of anti-noise quantum network coding protocol, where dotted lines rectangles represent Bell base measurements and solid rectangles represent joint measurements

Only the senders and receivers know the corresponding relations between four Pauli operators and 2-bit classical information. This paper defines four coding schemes as follows:

$$\begin{aligned}&Scheme\ 1\text{:}\ I\leftrightarrow 00,\ \sigma_Z\leftrightarrow 01,\ \sigma_X\leftrightarrow 10,\ i\sigma_Y\leftrightarrow 11,\\&Scheme\ 2\text{:}\ I\leftrightarrow 00,\ \sigma_Z\leftrightarrow 10,\ \sigma_X\leftrightarrow 01,\ i\sigma_Y\leftrightarrow 11,\\&Scheme\ 3\text{:}\ I\leftrightarrow 11,\ \sigma_Z\leftrightarrow 01,\ \sigma_X\leftrightarrow 10,\ i\sigma_Y\leftrightarrow 00,\\&Scheme\ 4\text{:}\ I\leftrightarrow 11,\ \sigma_Z\leftrightarrow 10,\ \sigma_X\leftrightarrow 01,\ i\sigma_Y\leftrightarrow 00.\end{aligned} \tag{9}$$

Pauli operators coding scheme and Bell states vector $|\varphi\rangle$ are determined randomly between S_1, S_2, T_1 and T_2 in advance, and they also share a set of secret keys. Two senders S_1 and S_2 share a pair of Bell states $|\varphi\rangle_{A,B}$, where S_1 has the particle A and S_2 has the particle B. S_1 and T_2, S_2 and T_1 share a pair of Bell states $|\varphi\rangle_{1,2}$ and $|\varphi\rangle_{3,4}$, respectively, where S_1 has the particle 1, T_2 has the particle 2, S_2 has the particle 3 and T_1 has the particle 4.

The protocol process can be described as follows:

S1) S_1 and S_2 determine the location of the particles in the message mode or control mode according to the key.

S2) (a) In the control mode, S_1 (S_2) sends the particle A (B) on hand directly to C_1, and then C_1 gets $|\varphi\rangle_{A,B}$.

(b) In the message mode, S_1 (S_2) applies U_{m1} (U_{m2}) on the particle A (B) and sends it ($|\varphi\rangle_{A',B'}$) to C_1 (C_1), at the same time, S_1 (S_2) applies U_{m1} (U_{m2}) on the particle 1(3) and sends it to T_2 (T_1).

S3) C_1 sends the particles $|\varphi\rangle_{A,B}$ (or $|\varphi\rangle_{A',B'}$) to C_2.

S4) C_2 prepares the particles $|\varphi\rangle_{A,B}$ (or $|\varphi\rangle_{A',B'}$) and sends them to T_1 and T_2 respectively.

S5) For particles in the control mode, T_1 and T_2 measured the obtained particles $|\varphi\rangle_{A,B}$ and compared with the initially determined Bell state carrier $|\varphi\rangle$. If the error rate is higher than a certain threshold, the communication will be abandoned. Otherwise, it turns to the Step S6).

S6) Let decode the information at node T_1 and T_2 respectively to obtain the classical information.

Where, at node T_2, we can get U_{m1} by perform the joint measurement on the particles 1 and 2. Then $U_{m1}U_{m2}$ can be obtained by measuring the Bell state $|\varphi\rangle_{A',B'}$ transmitted by C_2. Finally, we can get U_{m2} by comparing U_{m1} and $U_{m1}U_{m2}$, so that we can restore m_2. In the same way, we can decode m_1 at the node T_1.

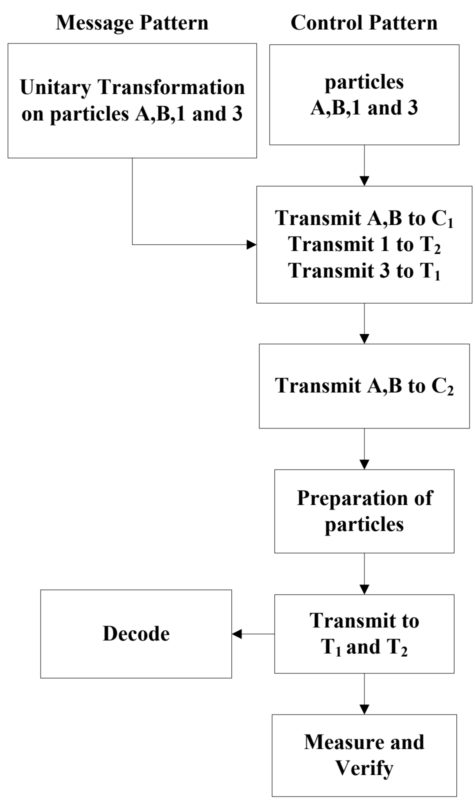

Figure 3: The new network coding protocol's process

For clarity, an example to illustrate the process of the message mode is given as follow.
Let suppose the scheme 1 in Eq. (9) is adopted as the coding method, and the Bell state carrier is the quantum state as Eq. (1). S_1 wants to transmit 00 to T_1, which is corresponding to the operation U_0, and S_2 wants to transmit 01 to T_2, which is corresponding to the operation U_1. S_1 and S_2 apply the unitary operations on the particle they have. As a result, C_1 gets $\left|\Phi^-\right\rangle_{A,B} = \frac{|00\rangle - |11\rangle}{\sqrt{2}}$. S_1 applies U_{m1} on the particle 1 and sends it to T_2, T_2 gets $\left|\Phi^+\right\rangle_{1,2} = \frac{|00\rangle + |11\rangle}{\sqrt{2}}$. In the same way, T_1 gets $\left|\Phi^-\right\rangle_{3,4} = \frac{|00\rangle - |11\rangle}{\sqrt{2}}$. Finally, T_1 gets $\left|\Phi^-\right\rangle_{3,4}$ and $\left|\Phi^-\right\rangle_{A,B}$, and T_2 gets $\left|\Phi^+\right\rangle_{1,2}$ and $\left|\Phi^-\right\rangle_{A,B}$. Finally, T_2 compares the results measured by $\left|\Phi^-\right\rangle_{A,B}$ and $\left|\Phi^+\right\rangle_{1,2}$ to obtain $U_{m1} = \sigma_Z$ and gets the information ***01***. By using the same method, T_1 can get the information ***00***.

4 Analysis of noise and fidelity

4.1 Quantum channel noises

Figures In this section, four noise environments in quantum channel will be illustrated, as well as the fidelity of the channels under the influence of four classical quantum noises, the bit-flip, phase-flip, amplitude damping and depolarizing noises.

Let suppose that the information carrier is $\left|\Phi^+\right\rangle = \frac{|00\rangle + |11\rangle}{\sqrt{2}}$, and the operations corresponding to the two bits of classical information transmitted by S_1 and S_2 are $U_{m1} = U_{m2} = I$.

The information carrier becomes $|\varphi\rangle_{A,B} = \frac{|00\rangle + |11\rangle}{\sqrt{2}}$ after performing the unitary operators of U_{m1} and U_{m2}. Its density matrix is given as follow:

$$\rho_0 = |\varphi\rangle\langle\varphi| = \frac{(|00\rangle + |11\rangle)(\langle 00| + \langle 11|)}{2} \tag{10}$$

The influence of noise environments on the quantum bit is usually representation with the sum of the operators. The operators E_k representing specific noise types are usually called Kraus operators satisfying

$$\sum_i E_i^+ E_i = I \tag{11}$$

The corresponding noise effect on the quantum bit k can be expressed as

$$\rho_k \to \rho'_k = \sum_i E_i^k \rho E_i^{k+} \tag{12}$$

After that the quantum bit is affected by the noise, the density matrix becomes

$$\rho \to \rho' = \sum_i E_i(p_A)[\sum_j F_j(p_B)\rho F_j^+(p_B)]E_i^+(p_A)$$
$$= \sum_i \sum_j E_{ij}(p_A, p_B)\rho E_{ij}^+(p_A, p_B). \quad (13)$$

Its fidelity is defined as

$$F = \langle \varphi | \rho' | \varphi \rangle \quad (14)$$

Here, $E_i(p_k)$ means that the operator E_i affects on the particle k, while $E_{ij}(p_A, p_B) = E_i(p_A) \otimes F_j(p_B)$, $E_i(p_A) = E_i(p_A) \otimes I$, $F_j(p_B) = I \otimes F_j(p_B)$.

4.1.1 Bit-flip noise

The bit-flip noise converts a quantum bit from $|0\rangle$ to $|1\rangle$ or from $|1\rangle$ to $|0\rangle$ with probability $p(0 \le p \le 1)$, whose Kraus operator can be expressed as follows:

$$E_0 = \sqrt{1-P}I, E_1 = \sqrt{P}\sigma_X \quad (15)$$

The density matrix at the node C_1 is

$$\rho_1 = \sum_i E_i(p_A)[\sum_j E_j(p_B)\rho_0 E_j^+(p_B)]E_i^+(p_A)$$
$$= \frac{1}{2}[(2p^2 - 2p + 1)(|00\rangle + |11\rangle)(\langle 00| + \langle 11|) \quad (16)$$
$$+(2p - 2p^2)(|01\rangle + |10\rangle)(\langle 01| + \langle 10|)]$$

Here, σ_X is the Pauli operator and Eq. (16) satisfies $i, j = 0,1$.

The density matrix at the node C_2 is given as

$$\rho_2 = \sum_i E_i(p_A)[\sum_j E_j(p_B)\rho_1 E_j^+(p_B)]E_i^+(p_A)$$
$$= \frac{1}{2}[(8p^4 - 16p^3 + 12p^2 - 4p + 1)(|00\rangle + |11\rangle)(\langle 00| + \langle 11|) \quad (17)$$
$$+(-8p^4 + 16p^3 - 12p^2 + 4p)(|01\rangle + |10\rangle)(\langle 01| + \langle 10|)]$$

The fidelity at the node C_2 is

$$F_{BF1} = \langle \varphi | \rho_2 | \varphi \rangle = 8p^4 - 16p^3 + 12p^2 - 4p + 1 \quad (18)$$

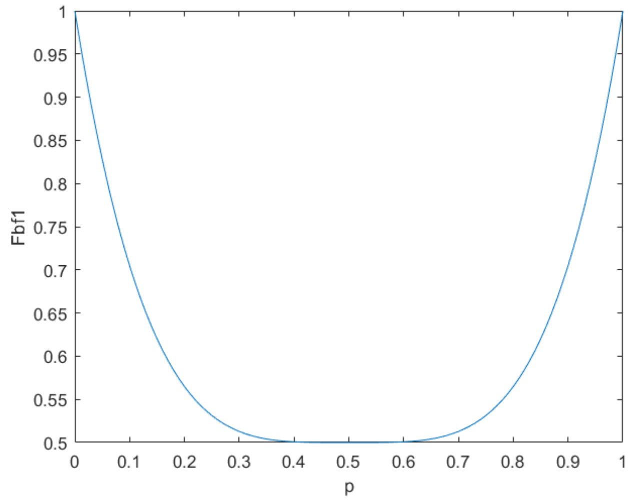

Figure 4: The fidelity of the channel at the node C_1 in the bit-flip noise

The Bell state is prepared at the node C_2 and then transmitted to T_1 and T_2. The fidelity of the node T_1 and T_2 compared to the node C_2 is

$$F_{BF2} = \langle \varphi | \rho_1 | \varphi \rangle = 2p^2 - 2p + 1 \tag{19}$$

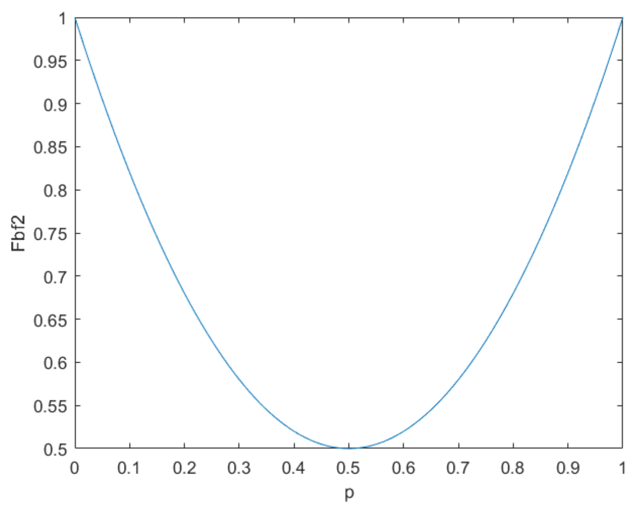

Figure 5: The channel fidelity of the destination node to node C_2 in the bit-flip noise

The fidelity of the whole transmission process is

$$F_{BF} = F_{BF1} \times F_{BF2} = 16p^6 - 48p^5 + 64p^4 - 48p^3 + 22p^2 - 6p + 1 \tag{20}$$

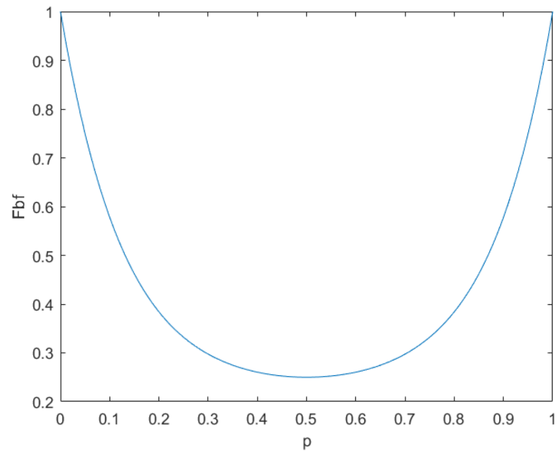

Figure 6: The fidelity of the whole channel in the bit-flip noise

According to the analysis results above, the effect of bit-flip noise has symmetry. When the noise probability $p = 0.5$, the channel has the lowest fidelity. When $0 \le p \le 0.5$, the channel fidelity decreases as the probability increases. When $0.5 \le p \le 1$, the fidelity of channel increases with the decrease of p.

4.1.2 Figure labels and captions

Figure labels must be sized in proportion to the image, sharp, and legible. Label size should be no smaller than 8-point and no larger than the font size of the main text. Labels must be saved using standard fonts (Arial, Helvetica or Symbol font) and should be consistent for all the figures. All labels should be in black, and should not be overlapped, faded, broken or distorted. A space must be inserted before measurement units. The first letter of each phrase, NOT each word, must be capitalized.

The phase-flip noise turns a quantum bit from $|1\rangle$ to $-|1\rangle$ with probability $p(0 \le p \le 1)$, the Kraus operator can be expressed as follows:

$$E_0 = \sqrt{1-P}I, E_1 = \sqrt{P}\sigma_Z \tag{21}$$

The density matrix at the node C_1 is:

$$\begin{aligned}\rho_1 &= \sum_i E_i(p_A)[\sum_j E_j(p_B)\rho_0 E_j^+(p_B)]E_i^+(p_A) \\ &= \frac{1}{2}[(2p^2-2p+1)(|00\rangle+|11\rangle)(\langle 00|+\langle 11|) \\ &+(2p-2p^2)(|00\rangle-|11\rangle)(\langle 00|-\langle 11|)]\end{aligned} \tag{22}$$

Here, σ_Z is the Pauli operator and Eq. (22) satisfies $i, j = 0,1$.

The density matrix at the node C_2 is

$$\rho_2 = \sum_i E_i(p_A)[\sum_j E_j(p_B)\rho_1 E_j^+(p_B)]E_i^+(p_A)$$
$$= \frac{1}{2}[(8p^4 - 16p^3 + 12p^2 - 4p + 1)(|00\rangle + |11\rangle)(\langle 00| + \langle 11|) \tag{23}$$
$$+(-8p^4 + 16p^3 - 12p^2 + 4p)(|00\rangle - |11\rangle)(\langle 00| - \langle 11|)]$$

The fidelity at the node C_2 is

$$F_{PF1} = \langle\varphi|\rho_2|\varphi\rangle = 8p^4 - 16p^3 + 12p^2 - 4p + 1 \tag{24}$$

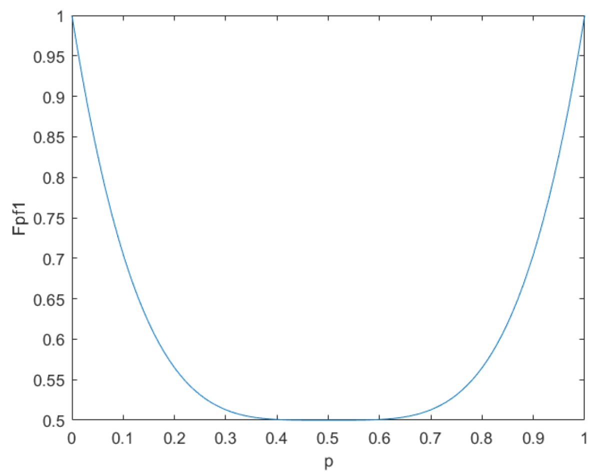

Figure 7: The fidelity of the channel at the node C_1 in the phase-flip noise

The Bell state is prepared at the node C_2 and then transmitted to T_1 and T_2. Then, the fidelity of the node T_1 and T_2 compared to that of the node C_2 is

$$F_{PF2} = \langle\varphi|\rho_1|\varphi\rangle = 2p^2 - 2p + 1 \tag{25}$$

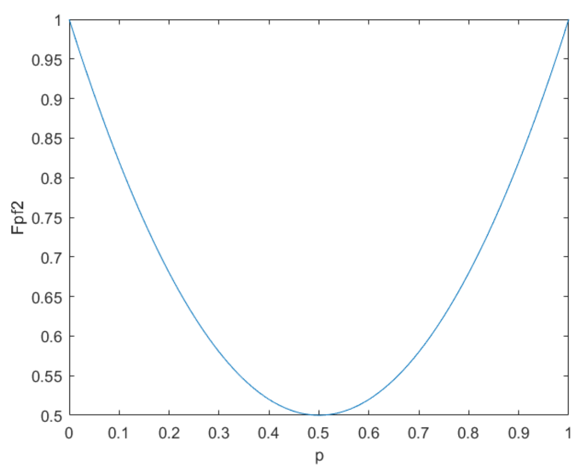

Figure 8: The channel fidelity of the destination node to node C_2 in the phase-flip noise

The fidelity of the whole transmission process is

$$F_{PF} = F_{PF1} \times F_{PF2} = 16p^6 - 48p^5 + 64p^4 - 48p^3 + 22p^2 - 6p + 1 \quad (26)$$

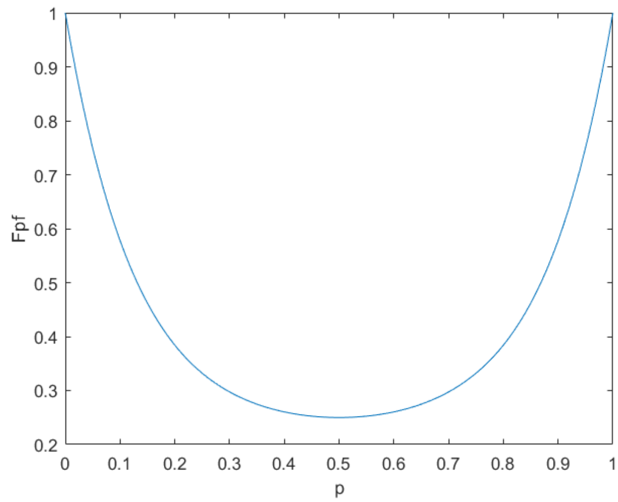

Figure 9: The fidelity of the whole channel in the phase-flip noise

According to the analysis results above, the effect of phase-flip noise has symmetry. When the noise probability $p = 0.5$, the channel has the lowest fidelity. When $0 \le p \le 0.5$, the channel fidelity decreases as p increases, when $0.5 \le p \le 1$, the fidelity of channel increases with the decrease of p. It is not difficult to find that the effect of bit-flip noise and the effect of phase-flip noise on the channel is the same. When the noise probability exceeds 0.5, the fidelity is enhanced instead, indicating that this channel has good resistance to strong bit-flip noise and strong phase-flip noise, which is very suitable to use in such an environment.

4.1.3 Amplitude damping

The amplitude damping noise denotes the loss of information due to energy decay, whose probability of a recession is $p(0 \le p \le 1)$. The Kraus operator can be expressed as follows:

$$E_0 = \begin{pmatrix} 1 & 0 \\ 0 & \sqrt{1-P} \end{pmatrix}, E_1 = \begin{pmatrix} 0 & \sqrt{P} \\ 0 & 0 \end{pmatrix} \quad (27)$$

The density matrix at the node C_1 is

$$\begin{aligned} \rho_1 &= \sum_i E_i(p_A)[\sum_j E_j(p_B)\rho_0 E_j^+(p_B)]E_i^+(p_A) \\ &= \frac{1}{2}[(|00\rangle + (1-p)|11\rangle)(\langle 00| + (1-p)\langle 11|) \\ &+ p(1-p)|10\rangle\langle 10| + p(1-p)|01\rangle\langle 01| + p^2|00\rangle\langle 00|] \end{aligned} \quad (28)$$

Here, Eq. (28) satisfies $i, j = 0,1$.

The density matrix at the node C_2 is

$$\rho_2 = \sum_i E_i(p_A)[\sum_j E_j(p_B)\rho_1 E_j^+(p_B)]E_i^+(p_A)$$
$$= \frac{1}{2}[|00\rangle + (1-p)^2|11\rangle)(\langle 00| + (1-p)^2\langle 11|)$$
$$+(-p^4 + 4p^3 - 5p^2 + 2p)|10\rangle\langle 10| \quad (29)$$
$$+(-p^4 + 4p^3 - 5p^2 + 2p)|01\rangle\langle 01|$$
$$+(p^4 - 4p^3 + 4p^2)|00\rangle\langle 00|]$$

The fidelity at the node C_2 is

$$F_{AD1} = \langle\varphi|\rho_2|\varphi\rangle = \frac{1}{2}p^4 - 2p^3 + 3p^2 - 2p + 1 \quad (30)$$

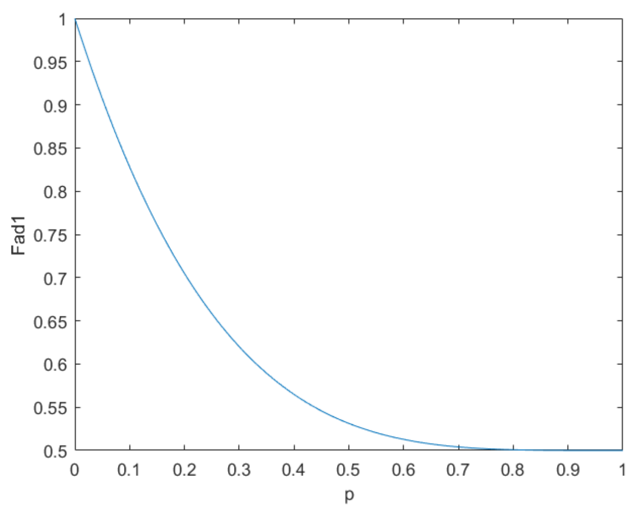

Figure 10: The fidelity of the channel at the node C_1 in the amplitude damping noise

The Bell state is prepared at the node C_2 and then transmitted to T_1 and T_2. Then, the fidelity of the node T_1 and T_2 compared to that of the node C_2 is

$$F_{AD2} = \langle\varphi|\rho_1|\varphi\rangle = \frac{1}{4}p^2 - p + 1 \quad (31)$$

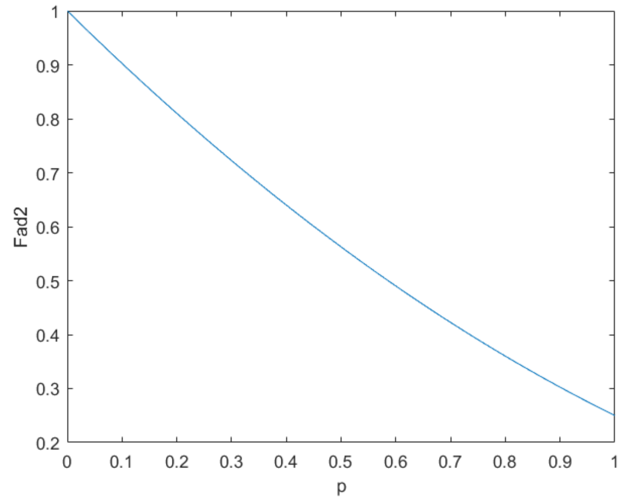

Figure 11: The channel fidelity of the destination node to node C_2 in the amplitude damping noise

The fidelity of the whole transmission process is

$$F_{AD} = F_{AD1} \times F_{AD2} = \frac{1}{8}p^6 - p^5 + \frac{13}{4}p^4 - \frac{11}{2}p^3 + \frac{21}{4}p^2 - 3p + 1 \tag{32}$$

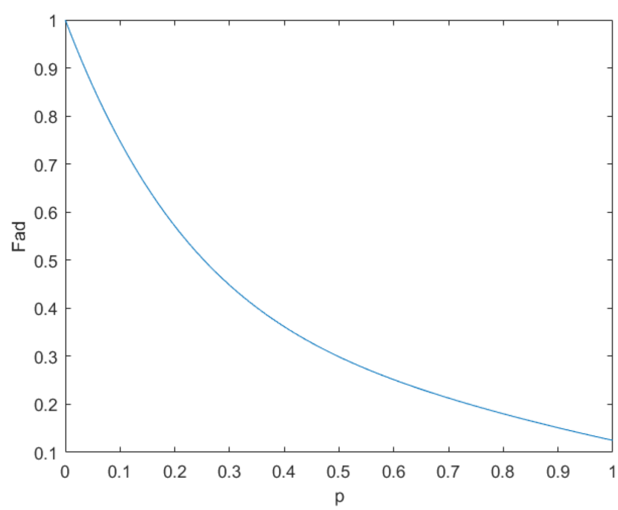

Figure 12: The fidelity of the whole channel in the amplitude damping noise

According to the analysis results above, the channel fidelity decreases as the probability decreases.

4.1.4 Depolarizing noise

The depolarizing noise usually makes the quantum bit replaced by a fully mixed state with probability $p(0 \le p \le 1)$, and makes the quantum bit remain the same with probability $1-p$. Its Kraus operator can be expressed as follows:

$$\begin{aligned} &E_0 = \sqrt{1-p}I, E_1 = \sqrt{\frac{p}{3}}\sigma_X \\ &E_2 = \sqrt{\frac{p}{3}}\sigma_Z, E_3 = \sqrt{\frac{p}{3}}\sigma_Y \end{aligned} \tag{33}$$

The density matrix at the node C_1 is

$$\begin{aligned} \rho_1 &= \sum_i E_i(p_A)[\sum_j E_j(p_B)\rho_0 E_j^+(p_B)]E_i^+(p_A) \\ &= \frac{1}{2}[(\frac{4}{3}p^2 - 2p + 1)(|00\rangle + |11\rangle)(\langle 00| + \langle 11|) \\ &+(-\frac{4}{9}p^2 + \frac{2}{3}p)(|00\rangle - |11\rangle)(\langle 00| - \langle 11|) \\ &+(-\frac{4}{9}p^2 + \frac{2}{3}p)(|01\rangle + |10\rangle)(\langle 01| + \langle 10|) \\ &+(-\frac{4}{9}p^2 + \frac{2}{3}p)(|01\rangle - |10\rangle)(\langle 01| - \langle 10|)] \end{aligned} \tag{34}$$

Here, σ_X, σ_Z and σ_Y are the Pauli operators and Eq. (34) satisfies $i, j = 0,1,2,3$.

The density matrix at the node C_2 is

$$\begin{aligned} \rho_2 &= \sum_i E_i(p_A)[\sum_j E_j(p_B)\rho_1 E_j^+(p_B)]E_i^+(p_A) \\ &= \frac{1}{2}[(\frac{46}{27}p^4 - \frac{64}{9}p^3 + 8p^2 - 4p + 1)(|00\rangle + |11\rangle)(\langle 00| + \langle 11|) \\ &+(-\frac{64}{81}p^4 + \frac{64}{27}p^3 - \frac{24}{9}p^2 + \frac{4}{3}p)(|00\rangle - |11\rangle)(\langle 00| - \langle 11|) \\ &+(-\frac{64}{81}p^4 + \frac{64}{27}p^3 - \frac{24}{9}p^2 + \frac{4}{3}p)(|01\rangle + |10\rangle)(\langle 01| + \langle 10|) \\ &+(-\frac{64}{81}p^4 + \frac{64}{27}p^3 - \frac{24}{9}p^2 + \frac{4}{3}p)(|01\rangle - |10\rangle)(\langle 01| - \langle 10|)] \end{aligned} \tag{35}$$

The fidelity at the node C_2 is

$$F_{D1} = \langle \varphi | \rho_2 | \varphi \rangle = \frac{64}{27}p^4 - \frac{64}{9}p^3 + 8p^2 - 4p + 1 \tag{36}$$

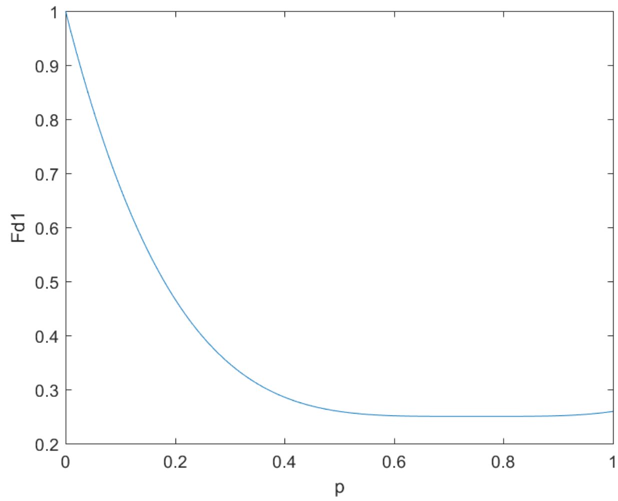

Figure 13: The fidelity of the channel at the node C_1 in the depolarizing noise

The Bell state is prepared at the node C_2 and then transmitted to T_1 and T_2. Then, the fidelity of the node T_1 and T_2 compared to that of the node C_2 is

$$F_{D2} = \langle\varphi|\rho_1|\varphi\rangle = \frac{4}{3}p^2 - 2p + 1 \tag{37}$$

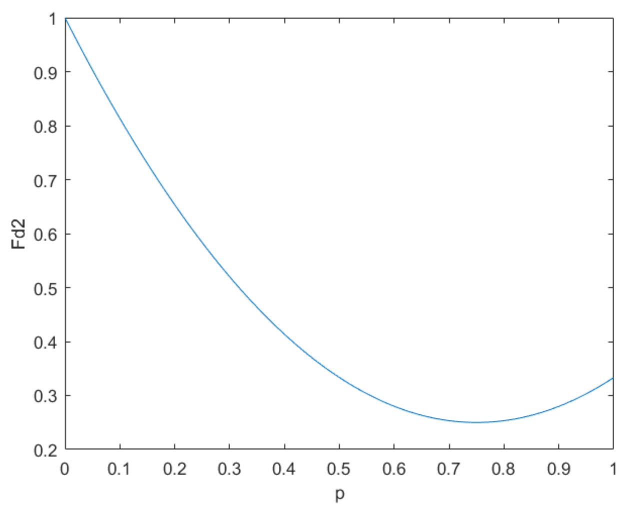

Figure 14: The channel fidelity of the destination node to node C_2 in the depolarizing noise

The fidelity of the whole transmission process is

$$F_D = F_{D1} \times F_{D2} = \frac{256}{81}p^6 - \frac{128}{9}p^5 + \frac{736}{27}p^4 - \frac{256}{9}p^3 + \frac{52}{3}p^2 - 6p + 1 \tag{38}$$

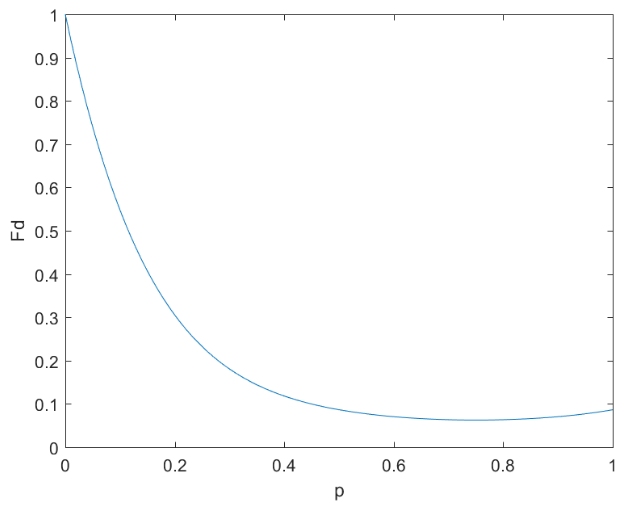

Figure 15: The fidelity of the whole channel in the depolarizing noise

According to the analysis results above, channel fidelity increases with probability. If $0 \le p \le 0.3$, the channel fidelity decreases sharply with the decreasing probability. If $0.3 \le p \le 0.8$, the fidelity decreases slowly with the decreasing probability. If $p > 0.8$, the fidelity of the channel is steepened again as the probability decreases.

4.2 Comparison of four noise effects

Tables Comparison of channel fidelity under the influence of four kinds of noise is shown in Fig. 16.

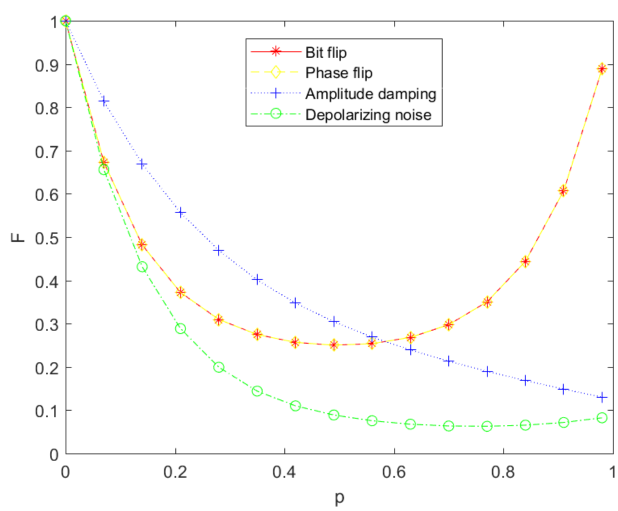

Figure 16: The comparison of four noise effects

It can be seen from Fig. 15 that when the noise probability $p \le 0.6$, the comparison of four kinds of noise's fidelity of the channel indicate that the amplitude damping has the least impact, the depolarizing noise has the largest impact, and the bit-flip noise and phase-flip noise have the same impact on the channel between that of the amplitude damping and that of the depolarizing noise. In the case of the probability of noise $p > 0.6$, the fidelity of bit-flip and phase-flip increases with the increase of noise probability. It means that they have good resistance to strong noise, and is very suitable to use in this noise environment.

5 Security and resource consumption analysis

The analytical results present following show that the novel protocol a good performance on security. The encoding agreement of U_x and option of Bell states can be viewed as the key for message transmission, which is only visible to the senders and the receivers. Provided that the attacker Eve carries out the intercept attack, he can eavesdrop to obtain all the information received by T_2. However, the only thing he get is the unitary operator, for the reason that he does not know the corresponding relationship between the four Pauli operators and the classical information, the attacker cannot get the message m_2 which is send to T_2 by S_2. In addition, the attacker cannot get the information sent by S_1 based on the information obtained by T_2, because he does not know which Bell state the sender uses as carrier and which Bell state the unitary operator is acted on. If Eve carries out the interception-retransmission attack, then he can make a Bell state randomly and send it to the destination node. In this case, the false Bell state obtained by the receiver can be detected with a certain probability. As a result, this communication will be abandoned to ensure the authenticity of the information received by the receiver.

In this protocol, the shared Bell entangled states between S_1 and T_2, S_2 and T_1 only plays an auxiliary role. So that, the new protocol accounts for a large part of the resource consumption. However, in the main transfer part, the consumption of resources is not very large.

6 Conclusions

In this paper, a novel quantum network coding protocol is proposed, which uses Bell states as the carrier to encode and transmit classical information by applying Pauli operators. The new algorithm cannot only realize the information transmission with better efficiency, but also effectively prevent potential eavesdropping attackers from obtaining information transmitted. By analyzing the influence of four kinds of noises on the quantum channel in this protocol, it is found that if the noise probability $p \le 0.6$, the amplitude damping noise has the least influence on the quantum channel, meanwhile the depolarizing noise has the greatest influence on the quantum channel. If the noise probability $p > 0.6$, the quantum channel has better resistance on bit flip and phase flip noises. Moreover, the protocol is possible to be combined with QSDC protocol or identity authentication mechanism to improve on the security performance of quantum network coding further.

Based on the detailed mathematical analysis to the efficiency and security, it can be concluded that the proposed protocol not only perform well on improving the efficiency of information transmission, throughput and link utilization in quantum network, but also on enhancing reliability and preventing eavesdropping attacks.

Acknowledgement: This work was supported in part by the National Natural Science Foundation of China under Grant Nos. 61373131, 61671087, 61601358, 61501247, 61672290, 61303039, and Grant 61232016, in part by the Six Talent Peaks Project of Jiangsu Province under Grant 2015-XXRJ-013, in part by the Natural Science Foundation of Jiangsu Province under Grant BK20171458, in part by the Natural Science Foundation of the Higher Education Institutions of Jiangsu Province, China, under Grant 16KJB520030, in part by the Sichuan Youth Science and Technique Foundation under Grant 2017JQ0048, in part by the NUIST Research Foundation for Talented Scholars under Grant 2015r014, in part by the PAPD, and in part by the CICAEET funds.

References

Akter, L.; Natarajan, B. (2009): Qos constrained resource allocation to secondary users in cognitive radio networks. *Computer Communications*, vol. 32, no. 18, pp. 1923-1930.

Bennett, C. H. (1992): Quantum cryptography using any two nonorthogonal states. *Physical Review Letters*, vol. 68, no. 21, pp. 3121.

Bennett, C. H.; Brassard, G. (1984): Quantum cryptography: Public key distribution and coin tossing. *Proceedings of IEEE International Conference on Computers Systems and Signal Processing*, vol. 175, pp. 175-179.

Bennett, C. H.; Brassard, G.; Crépeau, C.; Jozsa, R.; Peres, A. et al. (1993): Teleporting an unknown quantum state via dual classical and einstein-podolsky-rosen channels. *Physical Review Letters*, vol. 70, no. 13, pp. 1895-1899.

Fortes, R.; Rigolin, G. (2015): Fighting noise with noise in realistic quantum teleportation. *Physical Review A*, vol. 92, no. 1, 012338.

Guan, X. W.; Chen, X. B.; Wang, L. C.; Yang, Y. X. (2014): Joint remote preparation of an arbitrary two-qubit state in noisy environments. *International Journal of Theoretical Physics*, vol. 53, no. 7, pp. 2236-2245.

Hayashi, M. (2007): Prior entanglement between senders enables perfect quantum network coding with modification. *Physical Review A*, vol. 76 no. 4, pp. 538-538.

Hayashi, M.; Iwama, K.; Nishimura, H. (2007): Quantum network coding. *Conference on Theoretical Aspects of Computer Science*, pp. 610-621.

Iri, M. (1971): On an extension of the maximum flow minimum cut theorem to multicommodity flows. *Journal of the Operations Research Society of Japan*, vol. 13, pp. 129-135.

Korotkov, A. N.; Keane, K. (2010): Decoherence suppression by quantum measurement reversal. *Physical Review A*, vol. 81, no. 81, pp. 1334-1342.

Ma, S. Y.; Chen, X. B.; Luo, M. X.; Niu, X. X.; Yang, Y. X. (2010): Probabilistic quantum network coding of m-qudit states over the butterfly network. *Optics Communications*, vol. 283, no. 3, pp. 497-501.

Moroder, T.; Kleinmann, M.; Schindler, P.; Monz, T.; Gühne, O. et al. (2013):

Certifying systematic errors in quantum experiments. *Physical Review Letters*, vol. 110, no. 18, 180401.

Nishimura, H. (2013): Quantum network coding-How can network coding be applied to quantum information? *International Symposium on Network Coding*, pp. 1-5.

Peng, C. Z.; Yang, T.; Bao, X. H.; Zhang, J.; Pan, J. W. (2005): Experimental free-space distribution of entangled photon pairs over 13 km: towards satellite-based global quantum communication. *Physical Review Letters*, vol. 94, no. 15, 150501.

Shang, T.; Zhao, X. J.; Wang, C.; Liu, J. W. (2014): Controlled quantum network coding scheme based on single controller. *Acta Electronica Sinica*, vol. 42, no. 10, pp. 1913-1917.

Wang, M. M.; Qu, Z. G. (2016): Effect of quantum noise on deterministic joint remote state preparation of a qubit state via a GHZ channel. *Quantum Information Processing*, vol. 15, no. 11, pp. 4805-4818.

Wang, M. M.; Qu, Z. G.; Wang, W.; Chen, J. G. (2017): Effect of noise on joint remote preparation of multi-qubit state. *International Journal of Quantum Information*, vol. 15, no. 2, 1750012.

Wang, M. M.; Qu, Z. G.; Wang, W.; Chen, J. G. (2017): Effect of noise on deterministic joint remote preparation of an arbitrary two-qubit state. *Quantum Information Processing*, vol. 16, no. 5, pp. 140.

Wei, Y.; Cioffi, J. M. (2002): FDMA capacity of gaussian multiple-access channels with ISI. *IEEE Transactions on Communications*, vol. 50, no. 1, pp. 102-111.

Yan, S. S.; Kuang, H. M.; Guo, Y. (2012): Quantum coding of butterfly network based on controlled quantum teleportation. *National Scientific Paper Online Excellent Paper*, vol. 5, no. 20, pp. 1996-2001.

Yin, J.; Ren, J. G.; Lu, H.; Cao, Y.; Yong, H. L. et al. (2013): Quantum teleportation and entanglement distribution over 100-kilometre free-space channels. *Nature*, vol. 488, no. 7410, pp. 185-188.

Yu, S; Pan, J. W. (2014): I have a quantum dream in mind. *The People's Daily*.